Kumar G. Aditya (Orcid ID: 0000-0002-0708-3481)
Chattopadhyay Amitabha (Orcid ID: 0000-0002-2618-2565)

Late Endosomal/Lysosomal Accumulation of a Neurotransmitter Receptor in a Cellular Model of Smith-Lemli-Opitz Syndrome

Ashwani Sharma[1,2], G. Aditya Kumar[1,3], Amitabha Chattopadhyay[1,2,*]

[1]CSIR-Centre for Cellular and Molecular Biology, Uppal Road, Hyderabad 500 007, India
[2]Academy of Scientific and Innovative Research, Ghaziabad 201 002, India

Running title: Serotonin$_{1A}$ receptor trafficking in SLOS

Synopsis

Smith-Lemli-Opitz syndrome (SLOS) is an autosomal recessive disorder associated with defective cholesterol biosynthesis for which no specific drug is available yet. We report altered trafficking of the serotonin$_{1A}$ receptor (an important neurotransmitter receptor) in SLOS-mimicking conditions. We observed a reduction in plasma membrane population of the serotonin$_{1A}$ receptors under these conditions and an intracellular accumulation of the receptor in sterol-enriched late endosomal/lysosomal compartments. We believe that our results bring out novel physiological correlates in the molecular etiology of SLOS.

[3]Present address: Department of Pharmacology, University of Michigan Medical School, Ann Arbor, MI 48109, USA

*Address correspondence to Amitabha Chattopadhyay, Tel: +91-40-2719-2578, E-mail: amit@ccmb.res.in

This is the author manuscript accepted for publication and has undergone full peer review but has not been through the copyediting, typesetting, pagination and proofreading process, which may lead to differences between this version and the Version of Record. Please cite this article as doi: 10.1111/tra.12811

ABSTRACT

Smith-Lemli-Opitz syndrome (SLOS) is a congenital and developmental malformation syndrome associated with defective cholesterol biosynthesis. It is characterized by accumulation of 7-dehydrocholesterol (the immediate biosynthetic precursor of cholesterol in the Kandutsch-Russell pathway) and an altered cholesterol to total sterol ratio. Since SLOS is associated with neurological malfunction, exploring the function and trafficking of neuronal receptors and their interaction with membrane lipids under these conditions assume significance. In this work, we generated a cellular model of SLOS in HEK-293 cells stably expressing the human serotonin$_{1A}$ receptor (an important neurotransmitter G-protein coupled receptor) using AY 9944, an inhibitor for the enzyme 3β-hydroxy-steroid-Δ^7-reductase (7-DHCR). Using a quantitative flow cytometry based assay, we show that the plasma membrane population of serotonin$_{1A}$ receptors was considerably reduced under these conditions without any change in total cellular expression of the receptor. Interestingly, the receptors were trafficked to sterol-enriched LysoTracker positive compartments, which accumulated under these conditions. To the best of our knowledge, our results constitute one of the first reports demonstrating intracellular accumulation and misregulated traffic of a neurotransmitter GPCR in SLOS-like conditions. We believe these results assume relevance in our overall understanding of the molecular basis underlying the functional relevance of neurotransmitter receptors in SLOS.

KEYWORDS: AY 9944; cholesterol; 7-DHC; SLOS; serotonin$_{1A}$ receptor; altered trafficking

1 INTRODUCTION

The Smith-Lemli-Opitz syndrome (SLOS)[1] is a congenital error of cholesterol biosynthesis which results in developmental, behavioral and cognitive abnormalities.[2-5] SLOS is caused due to mutation(s) in the gene encoding 3β-hydroxy-steroid-Δ^7-reductase (7-DHCR), the enzyme which catalyzes the conversion of 7-dehydrocholesterol (7-DHC) to cholesterol in the last step of the Kandutsch-Russell pathway of cholesterol biosynthesis (Figure 1a).[6,7]

SLOS is relatively common in the Caucasian population with an estimated incidence between 1:10,000 and 1:70,000 and a carrier frequency of 1:30,[8,9] and more than 150 mutations in the gene (*DHCR7*) encoding 7-DHCR have been reported that lead to the disorder.[10] The affected patients exhibit anatomical defects such as syndactyly, polydactyly, cleft palate, microcephaly and abnormal gums. These developmental abnormalities are believed to be due to defective signaling of Sonic Hedgehog, the protein implicated in development and pattern formation.[11-13] SLOS is characterized by reduced levels of plasma cholesterol along with accumulation of 7-DHC and its positional isomer 8-dehydrocholesterol (8-DHC).[4] Interestingly, the ratio of these sterols to cholesterol has been reported to be linearly related to impairment in cognitive and adaptive function, with the amount of 7-DHC accumulation being the most important determinant.[5] Although learning and cognitive disabilities are well established for patients suffering from SLOS, the role of neuronal receptors and their interaction with membrane lipids in this context are relatively less explored.

Serotonin receptors are neurotransmitter receptors that belong to the superfamily of G protein-coupled receptors (GPCRs) and are implicated in the modulation of cognitive and behavioral functions.[14-16] The serotonin$_{1A}$ receptor is an important neurotransmitter receptor in the family of serotonin receptors and is implicated in a variety of cognitive, behavioral and developmental functions such as sleep, mood, aggression, anxiety and depression.[17-24] With an overall goal of understanding the mechanistic basis underlying the impaired neuronal

function observed in SLOS, we have previously shown that functional aspects of the serotonin$_{1A}$ receptor, such as ligand binding, G-protein coupling and cellular signaling, are affected in SLOS-like conditions.[25-28]

Extensive work over the past decade has highlighted the importance of spatiotemporal organization of GPCRs in their cellular function.[29-31] Although GPCRs have been classically considered to be plasma membrane resident signaling hubs, their subcellular localization has emerged as an important feature associated with regulation of their function.[32-34] This raises an interesting possibility of changes in cellular localization of GPCRs such as the serotonin$_{1A}$ receptor in disorders such as SLOS. In this work, we have monitored the subcellular localization and trafficking of the serotonin$_{1A}$ receptor under SLOS-mimicking conditions. To achieve this, we generated a cellular model of SLOS in HEK-293 cells stably expressing N-terminal myc-tagged human serotonin$_{1A}$ receptors (HEK-5-HT$_{1A}$R cells) by metabolically inhibiting the last step in the Kandutsch-Russell pathway of cholesterol biosynthesis[35-37] using AY 9944, which inhibits the enzyme 7-DHCR.[26,38] Chronic treatment of cells with AY 9944 resulted in accumulation of 7-DHC and an altered cholesterol to total sterol ratio. We monitored plasma membrane population of the serotonin$_{1A}$ receptor under these conditions using a quantitative flow cytometry based assay recently developed by us.[39] Our results show a considerable reduction in the plasma membrane population of serotonin$_{1A}$ receptors in cells treated with AY 9944 without any change in the total cellular expression of the receptor. Interestingly, we observed a considerable increase in sterol-enriched LysoTracker positive compartments inside cells, with accumulation of serotonin$_{1A}$ receptors in these compartments in SLOS-mimicking conditions. These results point toward an altered trafficking regime of the serotonin$_{1A}$ receptor in these conditions. To the best of our knowledge, our results constitute one of the first reports demonstrating intracellular accumulation and misregulated traffic of a GPCR in SLOS-like conditions. From a broader perspective, these results contribute to our overall understanding of the molecular basis underlying receptor trafficking under conditions of defective sterol biosynthesis.

2 RESULTS

2.1 Generating a cellular model of Smith-Lemli-Opitz syndrome

We previously showed that serotonin$_{1A}$ receptors stably expressed in HEK-5-HT$_{1A}$R cells exhibit characteristic ligand binding and G-protein coupling, and undergo clathrin-mediated endocytosis upon agonist stimulation.[39] In this work, with an overall goal of understanding the role of membrane lipids in trafficking of the serotonin$_{1A}$ receptor and its implications in health and disease, we developed a cellular model of SLOS in HEK-5-HT$_{1A}$R cells. For this, we used AY 9944,[38] a specific metabolic inhibitor which inhibits the enzyme (7-DHCR) that catalyzes the conversion of 7-DHC to cholesterol in the last step of the Kandutsch-Russell pathway of cholesterol biosynthesis (Figure 1a).[35-37] Notably, AY 9944 has been extensively utilized for mimicking SLOS in cellular and animal models.[40-42] We chose AY 9944 concentrations carefully to ensure that cellular viability was not affected under our experimental conditions, as determined by 3-(4,5-dimethylthiazol-2-yl)-2,5-diphenyl-tetrazolium bromide (MTT) assay (Figure 1b). SLOS is characterized by accumulation of 7-DHC accompanied by an altered cholesterol to total sterol ratio. In order to validate the cellular model, we quantified cholesterol to total sterol ratio using thin layer chromatography (TLC) upon AY 9944 treatment (Figure 1c). Since 7-DHC could be converted to 8-DHC (the positional isomer of 7-DHC), the observed TLC band corresponding to the 7-DHC standard could be a combination of 7-DHC and 8-DHC and is often termed as DHC to indicate a combination of both dehydrocholesterol species. As shown in Figure 1c, we did not observe any band corresponding to 7-DHC standard under control condition. However, bands corresponding to 7-DHC standard could be visualized upon chronic treatment (66 h) with 2 and 4 μM AY 9944. Densitometric analysis of the TLC bands corresponding to 2 and 4 μM AY 9944 treatment showed cholesterol/total sterol ratio of 0.97 (Figure 1d). Notably, the ratio of sterols obtained upon AY 9944 treatment was comparable to cholesterol/total sterol ratios reported in SLOS patients.[43]

2.2 Reduction in plasma membrane serotonin$_{1A}$ receptor population under SLOS-like conditions without any change in its total cellular expression

We have previously shown that in normal condition, the serotonin$_{1A}$ receptor predominantly localizes on the plasma membrane in HEK-5-HT$_{1A}$R cells.[39] Since GPCRs are considered to be canonical plasma membrane resident receptors involved in signal transduction, we monitored the effect of SLOS-like conditions on the plasma membrane population of serotonin$_{1A}$ receptors using a quantitative flow cytometric assay, previously developed by us.[39] In this assay, we exclusively label the plasma membrane associated serotonin$_{1A}$ receptor population with anti-myc antibody Alexa Fluor 488 conjugate. Relative shifts in the flow cytometric histogram (quantified as mode count, which represents counts in the modal channel of the histogram) are indicative of changes in the plasma membrane receptor population (Figure 2a). We observed that upon treatment with AY 9944, there was considerable reduction in the plasma membrane population of the serotonin$_{1A}$ receptor. For example, upon treatment with 2 μM AY 9944 for 66 h, we observed ~42% reduction in the plasma membrane receptor population relative to control. Upon treatment with 4 μM AY 9944, the reduction in plasma membrane receptor population was ~64% (Figure 2b). These results show that the plasma membrane population of the serotonin$_{1A}$ receptor exhibits considerable reduction under SLOS-like conditions.

In order to explore whether the decrease in plasma membrane population of the serotonin$_{1A}$ receptor upon AY 9944 treatment was due to reduction in the overall expression of the receptor, we performed Western blot analysis from whole cell protein extract under control and AY 9944 treated conditions (Figure 2c). Upon quantitation using densitometric analysis of bands corresponding to the serotonin$_{1A}$ receptor, we did not observe any significant change in the total cellular expression of the receptor upon chronic treatment (66 h) with 2 and 4 μM AY 9944 (Figure 2d). Taken together with our observations on the reduction of the plasma membrane receptor population (Figures 2a,b), these results suggest a possible effect of SLOS-like conditions on trafficking of the serotonin$_{1A}$ receptor to the plasma membrane.

2.3 Accumulation of LysoTracker positive compartments upon AY 9944 treatment

Since SLOS is associated with cholesterol metabolism and lysosomes play a key role in regulating cellular distribution of cholesterol,[44,45] we measured cellular distribution of lysosomes using LysoTracker red which stains acidic compartments inside cells (*i.e.,* late endosomes/lysosomes). Notably, we found a considerable increase in LysoTracker red staining in cells treated with AY 9944 relative to control cells (Figure 3a). We further quantified LysoTracker red staining under these conditions using flow cytometry. We observed a significant increase in mean fluorescence intensity of LysoTracker red in AY 9944 treated cells relative to control condition (Figures 3b,c).

2.4 Serotonin$_{1A}$ receptor accumulates in LysoTracker positive compartments under SLOS-like conditions

To further explore the effect of increased LysoTracker positive compartments in SLOS-mimicking conditions, we tested whether serotonin$_{1A}$ receptors were trafficked to these compartments upon AY 9944 treatment. As shown in Figure 4a, we observed a significant increase in colocalization of serotonin$_{1A}$ receptors with LysoTracker in these conditions. We further measured the extent of colocalization using Manders' colocalization coefficient[46] upon chronic treatment (66 h) with 2 and 4 μM AY 9944, and observed a concentration-dependent increase in colocalization of the serotonin$_{1A}$ receptor with LysoTracker positive compartments (Figure 4b). These results point toward directed trafficking of serotonin$_{1A}$ receptors to late endosomal/lysosomal pools in SLOS-like conditions.

2.5 LysoTracker positive compartments are sterol enriched

Since SLOS is associated with defects in cellular cholesterol metabolism, we monitored the distribution of free sterol in AY 9944 treated conditions using filipin. Filipin is an intrinsically fluorescent polyene antibiotic which stains unesterified sterols and allows the study of cellular distribution of sterols.[47,48] We observed a significant increase in cellular filipin staining upon chronic treatment with AY 9944 (see Figure 5a). These results, combined with our observation of increased LysoTracker positive compartments, prompted us to monitor the colocalization of filipin with LysoTracker red. As shown in Figure 5a, there was

a visibly high overlap of filipin with LysoTracker red. Quantification of colocalization using Manders' colocalization coefficient exhibited significant increase in colocalization of filipin with LysoTracker red upon AY 9944 treatment (shown in Figure 5b). Taken together with our results shown in Figures 3 and 4, these observations show that under SLOS-like conditions, the serotonin$_{1A}$ receptor exhibits a novel trafficking pattern directed toward sterol-enriched late endosomal/lysosomal pools.

3 DISCUSSION

SLOS is an autosomal recessive disorder which is caused due to defective cholesterol biosynthesis.[1-5] SLOS is characterized by the accumulation of 7-DHC (the immediate biosynthetic precursor of cholesterol in the Kandutsch-Russell pathway) and an altered cholesterol to total sterol ratio.[6,7] Till date, there is no specific drug available to treat SLOS. Although some therapies are recommended by clinicians, none of them have gone through the rigor of a comprehensive clinical trial.[49] Owing to the developmental, behavioral and cognitive abnormalities associated with SLOS, the role of neuronal receptors in the etiology of the disorder assumes relevance. The serotonin$_{1A}$ receptor represents an important member of the neurotransmitter GPCR family involved in cognitive, behavioral and developmental functions, and therefore serves as an important target for the development of novel therapeutics in neuropathological conditions such as SLOS.[15,16,20-23] However, the mechanistic basis underlying the role of the serotonin$_{1A}$ receptor and its interaction with membrane lipids in SLOS is relatively less explored. In this context, previous work from our laboratory has demonstrated impaired ligand binding, G-protein coupling and cellular signaling by the serotonin$_{1A}$ receptor under SLOS-like conditions.[25-28] In this work, we show that the plasma membrane population of serotonin$_{1A}$ receptors exhibits a considerable reduction in a cellular model of SLOS generated by treating cells with AY 9944. Our results demonstrate a considerable increase in sterol-enriched LysoTracker positive compartments in

this condition, a hallmark of lysosomal storage disorders such as Niemann-Pick type C (NPC) disease.[45,50,51] In addition, our results show that serotonin$_{1A}$ receptors are trafficked to these compartments upon AY 9944 treatment, indicating an altered trafficking pathway associated with SLOS-mimicking conditions. Notably, accumulation of lysosomal inclusion bodies has been reported in fibroblasts obtained from SLOS patients.[52] At this point, we cannot rule out any possible contribution of lysosomal accumulation of AY9944 in the observed increase in sterol-enriched LysoTracker positive compartments, since AY9944 belongs to the family of cationic amphiphilic drugs (CAD).[53]

The accumulation of 7-DHC is an important clinical manifestation of SLOS[5] and most of the effects are believed to arise either from altered sterol ratios or due to derivatives of 7-DHC formed under these conditions. Although 7-DHC differs from cholesterol *merely* by the presence of an additional double bond at the 7th position in the sterol ring (marked by a red circle in Figure 1a), it exhibits differential effects on membrane physical properties. Cholesterol is known to fine-tune lipid-protein interactions by increasing the thickness of the membrane with increasing cholesterol content.[54] Such increase in membrane thickness along the endoplasmic reticulum-Golgi-plasma membrane pathway has been implicated in efficient sorting of membrane proteins and receptors.[55] What would be the effect on this process if we replace a fraction of membrane cholesterol with 7-DHC? Is 7-DHC as efficient in this process of organelle-specific lipid-protein interaction as cholesterol? It appears that 7-DHC is not as effective as cholesterol in increasing membrane thickness.[56,57] There are additional differences in physical properties between membranes containing 7-DHC and cholesterol. For example, it has been reported that membranes prepared from skin fibroblasts of SLOS patients display increased 7-DHC content and abnormal membrane fluidity.[58] In addition, membranes containing 7-DHC exhibit greater sterol tilt angle[56], membrane packing[59,60] and phase behavior[61,62] relative to membranes containing cholesterol. In this context, we have previously shown that 7-DHC differs from cholesterol in its ability to increase membrane dipole potential.[63,64] In a recent work, using fluorescence lifetime distribution analysis of a membrane interfacial probe, we demonstrated that membranes containing 7-DHC exhibit

reduced interfacial temporal heterogeneity relative to membranes containing cholesterol.[65] Such differential effects on membrane physical properties could affect function of membrane proteins.[25-27,55,66,67] Altered functioning of membrane proteins such as NPC1 owing to such changes in membrane properties could be a cause for secondary NPC-like storage defects observed in SLOS.[44]

Importantly, accumulation of exogenously derived (from LDL) free cholesterol has been previously reported in cultured fibroblasts from SLOS patients.[52] Such accumulation of free cholesterol could drive partitioning of serotonin$_{1A}$ receptors to these compartments. As discussed above, this is supported by the cholesterol-induced increase in membrane thickness observed along the membrane protein biosynthetic trafficking and sorting pathway.[55,68] Accumulation of additional compartments enriched in cholesterol could perturb the intracellular biosynthetic itinerary of membrane proteins such as serotonin$_{1A}$ receptors (Figure 6, proposed pathway 1). Another possibility is that the receptors could be re-routed during the course of constitutive internalization and recycling to the plasma membrane (Figure 6, proposed pathway 2). This is supported by reports in which cholesterol accumulation has been shown to cause a defect in late endosome motility and intra-endosomal trafficking.[69,70] Interestingly, slow recycling of transferrin receptors has been reported in NPC cells[71] and accumulation of endosomal cholesterol has been shown to affect recycling of transferrin in Niemann-Pick type A and C lipid storage disease fibroblasts.[72]

Defective trafficking of GPCRs has been implicated in diseases such as nephrogenetic diabetes insipidus, retinitis pigmentosa and cancer.[73-75] Recent work from our group has shown that statin-induced chronic cholesterol depletion affects the mechanism of endocytosis and the intracellular trafficking of the serotonin$_{1A}$ receptor.[76] In this overall context, our present results showing reduced plasma membrane localization of the serotonin$_{1A}$ receptor and its accumulation in sterol-enriched LysoTracker positive compartments highlight a novel trafficking defect associated with SLOS-like conditions. Looking ahead, the use of cellular systems expressing *DHCR7* harboring naturally occurring mutations observed in SLOS could serve as a genetic model to monitor the effects of the SLOS phenotype and the associated

functional aspects of neurotransmitter receptors. Although HEK-293 cells offer a convenient and extensively studied system to explore receptor trafficking, these cells may not represent a native environment for the serotonin$_{1A}$ receptor. It would be interesting to explore the effect of the SLOS phenotype on the trafficking of neurotransmitter receptors in a more native system. We envision that a detailed mechanistic exploration of such altered trafficking and localization of the serotonin$_{1A}$ receptor in SLOS-like conditions could be critical in the development of novel therapeutic interventions against SLOS.

4 MATERIALS AND METHODS

4.1 Materials

AY 9944 (Cat #: C5364), cholesterol, 7-DHC, Tris, EDTA, poly-L-lysine, glycine, penicillin, streptomycin, gentamycin sulfate, MTT, filipin and doxycycline were obtained from Sigma Chemical Co. (St. Louis, MO). DMEM/F-12 [Dulbecco's modified Eagle's medium/nutrient mixture F-12 (Ham) (1:1)], fetal bovine serum (FBS), LysoTracker red, β-tubulin loading control monoclonal antibody (BT7R) (Cat #: MA5-16308, RRID: AB_2537819), cholesterol esterase (obtained from Amplex^{TM} red cholesterol assay kit) and hygromycin B were from Invitrogen/Life technologies (Grand Island, NY). Bicinchoninic acid (BCA) reagent for protein estimation was from Pierce (Rockford, IL). Anti-myc tag antibody Alexa Fluor 488 conjugate (9E10) (Cat #: 16-308, RRID: AB_568801) and myc-tag (9B11) mouse mAb (Cat #: 2276S, RRID: AB_331783) were obtained from Millipore (Bedford, MA) and Cell Signaling Technology, Inc. (Danvers, MA), respectively. Methanol and precoated silica gel 60 thin layer chromatography plates were from Merck (Darmstadt, Germany). HRP goat anti-mouse IgG antibody (Cat #: 405306, RRID: AB_315009) was from BioLegend (San Diego, CA) and bovine serum albumin (BSA) was from Himedia Laboratories (Mumbai, India). Acetone and chloroform were from Spectrochem (Mumbai, India). *n*-Heptane and ethyl acetate were obtained from Sisco Research Laboratories (Mumbai, India). All other chemicals used were of the highest purity available. Water was purified through a Millipore (Bedford, MA) Milli-Q system and used throughout.

4.2 Methods

4.2.1 Cell culture

HEK-293 cells stably expressing N-terminal myc-tagged serotonin$_{1A}$ receptors (HEK-5-HT$_{1A}$R cells) were grown as described previously.[39] Briefly, cells were grown in DMEM/F-12 medium supplemented with 10% FBS, 60 μg/ml penicillin, 50 μg/ml streptomycin, 50 μg/ml gentamycin sulfate in a humidified atmosphere with 5% CO_2 at 37 °C. Hygromycin B (250 μg/ml) was used to select cells expressing the serotonin$_{1A}$ receptor. Receptor expression was induced with 1 μg/ml doxycycline 24 h prior to experiment.

4.2.2 Treatment with AY 9944

HEK-5-HT$_{1A}$R cells plated on poly-L-lysine coated dishes were treated with AY 9944 as described previously.[26] Stock solution of AY 9944 was prepared in water. Cells were incubated for 24 h after seeding followed by treatment with 2 and 4 μM AY 9944 for 66 h in DMEM/F-12 medium supplemented with 5% FBS, 60 μg/ml penicillin, 50 μg/ml streptomycin and 50 μg/ml gentamycin sulfate. Control cells were grown under identical conditions except treatment with AY 9944.

4.2.3 MTT viability assay

Cellular viability upon AY 9944 treatment was determined using MTT assay as described previously.[77] Cells were plated in a 96-well plate and treated with AY 9944. Subsequently, cells were incubated for 1 h at 37 °C with MTT prepared in serum-free DMEM/F-12 media at a final concentration of 0.5 mg/ml. The media was washed off and DMSO was added and kept for 10 min at room temperature (~23 °C) to dissolve the formazan crystals. Absorbance was measured at 560 nm using an EnSpire 2300 Multimode Plate Reader (Perkin Elmer, Waltham, MA).

4.2.4 Thin layer chromatography for estimation of sterols

Lipids were isolated from cellular lysates obtained from control and AY 9944 treated samples. Briefly, cells were scraped, collected in ice-cold PBS and sonicated (5 min with 15/30 sec on/off cycles) using a Sonics Vibra-Cell VCX 500 sonifier (Sonics & Materials Inc, Newton, CT) fitted with a titanium microtip. Cellular lysates were treated with 0.2 U/ml cholesterol esterase at 37 °C for 1 h to hydrolyze esterified cholesterol, if any. Total protein concentration in cell lysates was measured using BCA assay.[78] Lipids from cellular lysates were extracted according to the Bligh and Dyer method.[79] Lipids were dried under a stream of nitrogen at ~40 °C and kept under a high vacuum till further use. Sterol content in the lipid mixture under various treatment conditions was estimated by thin layer chromatography (TLC). Precoated silica gel TLC plates were impregnated with 3% (w/v) silver nitrate in methanol and activated at ~100 °C for 15 min. Samples for TLC were prepared by dissolving the dried lipids in chloroform/methanol (1:1, v/v) just before use. Sterols were separated using *n*-heptane/ethyl acetate (2:1, v/v) as a solvent system.[25,80] The TLC plate was sprayed with 10% (w/v) cupric sulfate solution containing 8% (v/v) orthophosphoric acid followed by charring at ~150 °C to visualize separated lipids. Cholesterol and 7-DHC bands were identified with the help of standards. TLC plates were scanned and sterol band intensities were estimated using densitometric analysis of the chromatogram using Adobe Photoshop CS3 (Adobe systems, San Jose, CA) software. To quantify sterol ratios, a calibration curve was plotted from TLC developed using a range of known cholesterol/7-DHC (mol/mol) standards (see Figure S1). Cholesterol/total sterol ratios in AY 9944 treated samples were evaluated using this calibration curve.

4.2.5 Flow cytometric analysis

Plasma membrane receptor population of serotonin$_{1A}$ receptors was monitored using a quantitative flow cytometric assay.[39] Briefly, cells were scraped subsequent to treatment and collected in ice-cold PBS. Cells were fixed using 4% (w/v) formaldehyde solution in PBS for 30 min and the plasma membrane serotonin$_{1A}$ receptor population was labeled using anti-myc antibody Alexa Fluor 488 conjugate (1:100 dilution) in PBS containing 2% serum for 1 h,

followed by washing and resuspending in PBS. Data were acquired using a Gallios flow cytometer (Beckman Coulter Inc., Brea, CA) and analyzed in Kaluza analysis software version 2.1. Data were collected for 10,000 cells by exciting Alexa Fluor 488 at 488 nm and emission was collected using a 525/40 nm bandpass filter. Change in mode count values upon AY 9944 treatment was analyzed with respect to control condition.

To quantify LysoTracker positive compartments, cells were incubated with 0.3 μM LysoTracker red in serum-free DMEM/F-12 for 30 min at 37 °C. Media was washed off and cells were scraped in ice-cold PBS, washed and resuspended in ice-cold PBS. Data were acquired using a BD LSRFortessa^{TM} flow cytometer (Becton Dickinson, Franklin Lakes, NJ). Data were collected by exciting LysoTracker red at 561 nm and emission was collected using 585/15 nm bandpass filter. Change in mean fluorescence intensity was analyzed with respect to control condition.

4.2.6 Western blot analysis of total cellular expression of serotonin$_{1A}$ receptors

Total cellular protein was extracted from control and AY 9944 treated cells using radioimmunoprecipitation assay (RIPA) lysis buffer in presence of protease inhibitor cocktail. Samples were prepared by incubating 20-40 μg protein in electrophoresis sample buffer for 30 min at 37 °C. Samples were loaded and separated on a 12% SDS-PAGE gel. The separated proteins were then transferred to a nitrocellulose membrane using a semi-dry transfer apparatus (Amersham Pharmacia Biotech, Little Chalfont, UK). The nitrocellulose membrane was blocked for non-specific binding sites using 5% (w/v) BSA prepared in Tris buffer saline containing 0.1% (v/v) Tween 20 (TBST) for 1 h at room temperature (~23 °C). The membrane was probed overnight at 4 °C with myc-tag mouse mAb (1:5,000 dilution) in 5% (w/v) BSA in TBST to detect serotonin$_{1A}$ receptors. The membrane was washed three times with TBST and probed with HRP goat anti-mouse IgG antibody (1:10,000 dilution) for 1 h at room temperature (~23 °C). Bands were detected using enhanced chemiluminescence detection reagent and imaged in Chemi-Smart 5000 chemiluminescence detection system (Vilber Lourmat, Marne-la-Vallée, France). β-tubulin was used as a loading control and the

membrane was probed using β-tubulin monoclonal antibody (1:5,000 dilution). Band intensities of serotonin$_{1A}$ receptors and β-tubulin were quantified by densitometric analysis using Adobe Photoshop CS3 (Adobe Systems, San Jose, CA) software. The intensities of the bands corresponding to serotonin$_{1A}$ receptors were normalized to β-tubulin band intensities.

4.2.7 Confocal fluorescence imaging

HEK-5-HT$_{1A}$R cells were plated on poly-L-lysine coated glass coverslips and were treated with AY 9944 as described above. Upon completion of AY 9944 treatment, cells were incubated with 0.3 μM LysoTracker red in serum-free DMEM/F-12 medium for 30 min at 37 °C and subsequently washed with ice-cold PBS. Cells were fixed using 4% (w/v) formaldehyde solution in PBS for 10 min at room temperature (~23 °C) and washed with ice-cold PBS. For filipin staining, cells fixed with formaldehyde were stained with 50 μg/ml filipin in PBS for 45 min at room temperature (~23 °C) in dark. Cells were washed with ice-cold PBS. For staining cellular serotonin$_{1A}$ receptor population, fixed cells (or subsequent to filipin staining of cells) were permeabilized with 0.05% (v/v) Triton X-100 (prepared in ice-cold PBS) for 5 min on ice. Cells were washed with ice-cold PBS 4-5 times and blocked using 2% (w/v) BSA for 15 min at room temperature (~23 °C). Cells were labeled with anti-myc antibody Alexa Fluor 488 conjugate (1:100 dilution) in PBS containing 2% BSA for 1 h at room temperature (~23 °C), followed by washing with ice-cold PBS and mounted in Vectashield® antifade mounting medium. Images of *z*-sections were acquired on a Zeiss LSM 880 confocal microscope (Jena, Germany) using a 63x/1.4 NA oil immersion objective under 1 airy condition with a fixed step size of 0.5 μm. LysoTracker red was excited at 543 nm and emission was collected between 566 and 690 nm. Serotonin$_{1A}$ receptors were imaged by exciting anti-myc antibody Alexa Fluor 488 conjugate at 488 nm and emission was collected between 490 and 543 nm. Filipin was imaged using excitation at 405 nm and emission was collected between 410 and 460 nm.

4.2.8 Quantifying colocalization

Two-channel confocal microscopic images were analyzed for colocalization using Manders' colocalization coefficient as described previously with some modifications.[39] Briefly, Manders' colocalization coefficient was calculated for *z*-sections spanning the entire cellular volume using automatic threshold values using the JACoP plug-in for ImageJ (National Institutes of Health, Bethesda, MD).

4.2.9 Statistical analysis

Significance levels were analyzed using Student's two-tailed unpaired *t*-test with 95% confidence interval using GraphPad Prism software (version 4.0, San Diego, CA). Plots were generated using OriginPro (version 2021b, OriginLab, Northampton, MA).

ACKNOWLEDGMENTS

This work was supported by SERB Distinguished Fellowship grant (Department of Science and Technology, Govt. of India) to A.C. and core support from CSIR-Centre for Cellular and Molecular Biology. A.S. thanks the Council of Scientific and Industrial Research (CSIR) for the award of a Senior Research Fellowship. G.A.K. was supported as a Senior Project Associate by a CSIR FBR grant to A.C. (MLP 0146). We thank Gunda Srinivas for help with acquiring flow cytometric data and Parijat Sarkar and Md. Jafurulla for useful discussions. We acknowledge members of the Chattopadhyay laboratory for critically reading the manuscript and for their comments and suggestions.

AUTHOR CONTRIBUTION

A.S. performed experiments; A.S. and G.A.K. analyzed data; G.A.K. and A.C. designed experiments; A.S., G.A.K. and A.C. wrote the manuscript; A.C. conceptualized the project, edited the manuscript, organized access to research facilities and funding, and provided overall supervision and mentoring.

CONFLICT OF INTEREST

The authors declare no competing financial interests.

REFERENCES

1. Smith DW, Lemli L, Opitz JM. A newly recognized syndrome of multiple congenital anomalies. *J. Pediatr.* 1964;64(2):210-217.
2. Waterham HR, Wanders RJA. Biochemical and genetic aspects of 7-dehydrocholesterol reductase and Smith-Lemli-Opitz syndrome. *Biochim. Biophys. Acta* 2000;1529(1-3):340-356.
3. Chattopadhyay A, Paila YD. Lipid-protein interactions, regulation and dysfunction of brain cholesterol. *Biochem. Biophys. Res. Commun.* 2007;354(3):627-633.
4. Porter FD. Smith-Lemli-Opitz syndrome: pathogenesis, diagnosis and management. *Eur. J. Hum. Genet.* 2008;16(5):535-541.
5. Thurm A, Tierney E, Farmer C, Albert P, Joseph L, Swedo S, Bianconi S, Bukelis I, Wheeler C, Sarphare G, Lanham D, Wassif CA, Porter FD. Development, behavior, and biomarker characterization of Smith-Lemli-Opitz syndrome: an update. *J. Neurodev. Disord.* 2016;8:12.
6. Irons M, Elias ER, Salen G, Tint GS, Batta AK. Defective cholesterol biosynthesis in Smith-Lemli-Opitz syndrome. *Lancet* 1993;341(8857):1414.
7. Tint GS, Irons M, Elias ER, Batta AK, Frieden R, Chen TS, Salen G. Defective cholesterol biosynthesis associated with the Smith-Lemli-Opitz Syndrome. *N. Engl. J. Med.* 1994;330(2):107-113.
8. Battaile KP, Battaile BC, Merkens LS, Maslen CL, Steiner RD. Carrier frequency of the common mutation IVS8-1G>C in DHCR7 and estimate of the expected incidence of Smith–Lemli–Opitz syndrome. *Mol. Genet. Metab.* 2001;72(1):67-71.
9. Porter FD, Herman GE. Malformation syndromes caused by disorders of cholesterol synthesis. *J. Lipid Res.* 2011;52(1):6-34.
10. Waterham HR, Hennekam RCM. Mutational spectrum of Smith-Lemli-Opitz syndrome. *Am. J. Med. Genet. C Semin. Med. Genet.* 2012;160C(4):263-284.

11. Mullor JL, Sánchez P, Ruiz i Altaba A. Pathways and consequences: Hedgehog signaling in human disease. *Trends Cell Biol.* 2002;12(12):562-569.
12. Koide T, Hayata T, Cho KWY. Negative regulation of Hedgehog signaling by the cholesterogenic enzyme 7-dehydrocholesterol reductase. *Development* 2006;133(12):2395-2405.
13. Blassberg R, Jacob J. Lipid metabolism fattens up Hedgehog signaling. *BMC Biol.* 2017;15(1):95.
14. A. Chattopadhyay, ed. Serotonin Receptors in Neurobiology. Boca Raton, FL: CRC Press; 2007.
15. Nichols DE, Nichols CD. Serotonin receptors. *Chem. Rev.* 2008;108(5):1614-1641.
16. Sarkar P, Mozumder S, Bej A, Mukherjee S, Sengupta J, Chattopadhyay A. Structure, dynamics and lipid interactions of serotonin receptors: excitements and challenges. *Biophys. Rev.* 2021;13:101-122.
17. Pucadyil TJ, Kalipatnapu S, Chattopadhyay A. The serotonin$_{1A}$ receptor: a representative member of the serotonin receptor family. *Cell. Mol. Neurobiol.* 2005;25(3-4):553-580.
18. Kalipatnapu S, Chattopadhyay A. Membrane organization and function of the serotonin$_{1A}$ receptor. *Cell. Mol. Neurobiol.* 2007;27(8):1097-1116.
19. Müller CP, Carey RJ, Huston JP, De Souza Silva MA. Serotonin and psychostimulant addiction: focus on 5-HT$_{1A}$-receptors. *Prog. Neurobiol.* 2007;81(3):133-178.
20. Lacivita E, Leopoldo M, Berardi F, Perrone R. 5-HT$_{1A}$ receptor, an old target for new therapeutic agents. *Curr. Top. Med. Chem.* 2008;8(12):1024-1034.
21. Akimova E, Lanzenberger R, Kasper S. The serotonin-1A receptor in anxiety disorders. *Biol. Psychiatry* 2009;66(7):627-635.
22. Fiorino F, Severino B, Magli E, Ciano A, Caliendo G, Santagada V, Frecentese F, Perissutti E. 5-HT$_{1A}$ receptor: an old target as a new attractive tool in drug discovery from CNS to cancer. *J. Med. Chem.* 2014;57(11):4407-4426.
23. Kaufman J, DeLorenzo C, Choudhury S, Parsey RV. The 5-HT$_{1A}$ receptor in major depressive disorder. *Eur. Neuropsychopharmacol.* 2016;26(3):397-410.

24. Sarkar P, Kumar GA, Pal S, Chattopadhyay A. Biophysics of serotonin and the serotonin$_{1A}$ receptor: fluorescence and dynamics. In: Pilowsky PM, ed. Serotonin: the mediator that spans evolution. Amsterdam: Elsevier; 2018:3-22.

25. Singh P, Paila YD, Chattopadhyay A. Differential effects of cholesterol and 7-dehydrocholesterol on the ligand binding activity of the hippocampal serotonin$_{1A}$ receptor: implications in SLOS. *Biochem. Biophys. Res. Commun.* 2007;358(2):495-499.

26. Paila YD, Murty MRVS, Vairamani M, Chattopadhyay A. Signaling by the human serotonin$_{1A}$ receptor is impaired in cellular model of Smith-Lemli-Opitz syndrome. *Biochim. Biophys. Acta* 2008;1778(6):1508-1516.

27. Chattopadhyay A, Paila YD, Jafurulla M, Chaudhuri A, Singh P, Murty MRVS, Vairamani M. Differential effects of cholesterol and 7-dehydrocholesterol on ligand binding of solubilized hippocampal serotonin$_{1A}$ receptors: implications in SLOS. *Biochem. Biophys. Res. Commun.* 2007;363(3):800-805.

28. Sarkar P, Jafurulla M, Bhowmick S, Chattopadhyay A. Structural stringency and optimal nature of cholesterol requirement in the function of the serotonin$_{1A}$ receptor. *J. Membr. Biol.* 2020;253(5):445-457.

29. Lohse MJ, Hofmann KP. Spatial and temporal aspects of signaling by G-protein-coupled receptors. *Mol. Pharmacol.* 2015;88(3):572-578.

30. Thomsen ARB, Jensen DD, Hicks GA, Bunnett NW. Therapeutic targeting of endosomal G-protein-coupled receptors. *Trends Pharmacol. Sci.* 2018;39(10):879-891.

31. Lobingier BT, von Zastrow M. When trafficking and signaling mix: how subcellular location shapes G protein-coupled receptor activation of heterotrimeric G proteins. *Traffic* 2019;20(2):130-136.

32. Jong Y-JI, Harmon SK, O'Malley KL. GPCR signaling from within the cell. *Br. J. Pharmacol.* 2018;175(21):4026-4035.

33. Eichel K, von Zastrow M. Subcellular organization of GPCR signaling. *Trends Pharmacol. Sci.* 2018;39(2):200-208.

34. Crilly SE, Puthenveedu MA. Compartmentalized GPCR signaling from intracellular membranes. *J. Membr. Biol.* 2021;254(3):259-271.

35. Kandutsch AA, Russell AE. Preputial gland tumor sterols III. A metabolic pathway from lanosterol to cholesterol. *J. Biol. Chem.* 1960;235(8):2256-2261.

36. Nes WD. Biosynthesis of cholesterol and other sterols. *Chem. Rev.* 2011;111(10): 6423-6451.

37. Brown AJ, Sharpe LJ. Cholesterol synthesis. In: Ridgway ND, McLeod RS, eds. Biochemistry of Lipids, Lipoproteins and Membranes. Amsterdam: Elsevier; 2016: 327-358.

38. Dvornik D, Kraml M, Dubuc J, Givner M, Gaudry R. A novel mode of inhibition of cholesterol biosynthesis. *J. Am. Chem. Soc.* 1963;85(20):3309.

39. Kumar GA, Sarkar P, Jafurulla M, Singh SP, Srinivas G, Pande G, Chattopadhyay A. Exploring endocytosis and intracellular trafficking of the human serotonin$_{1A}$ receptor. *Biochemistry* 2019;58(22):2628-2641.

40. Kolf-Clauw M, Chevy F, Wolf C, Siliart B, Citadelle D, Roux C. Inhibition of 7-dehydrocholesterol reductase by the teratogen AY9944: a rat model for Smith-Lemli-Opitz syndrome. *Teratology* 1996;54(3):115-125.

41. Kapphahn RJ, Richards MJ, Ferrington DA, Fliesler SJ. Lipid-derived and other oxidative modifications of retinal proteins in a rat model of Smith-Lemli-Opitz syndrome. *Exp. Eye Res.* 2019;178:247-254.

42. Rao SR, Pfeffer BA, Gómez NM, Skelton LA, Keiko U, Sparrow JR, Rowsam AM, Mitchell CH, Fliesler SJ. Compromised phagosome maturation underlies RPE pathology in cell culture and whole animal models of Smith-Lemli-Opitz syndrome. *Autophagy* 2018;14(10):1796-1817.

43. Elias ER, Hansen RM, Irons M, Quinn NB, Fulton AB. Rod photoreceptor responses in children with Smith-Lemli-Opitz syndrome. *Arch. Ophthalmol*. 2003;121(12):1738-1743.

44. Platt FM, Wassif C, Colaco A, Dardis A, Lloyd-Evans E, Bembi B, Porter FD. Disorders of cholesterol metabolism and their unanticipated convergent mechanisms of disease. *Annu. Rev. Genomics Hum. Genet.* 2014;15:173-194.

45. Meng Y, Heybrock S, Neculai D, Saftig P. Cholesterol handling in lysosomes and beyond. *Trends Cell Biol.* 2020;30(6):452-466.

46. Manders EMM, Verbeek FJ, Aten JA. Measurement of co-localization of objects in dual-colour confocal images. *J. Microsc.* 1993;169:375-382.

47. Norman AW, Demel RA, de Kruyff B, van Deenen LL. Studies on the biological properties of polyene antibiotics. Evidence for the direct interaction of filipin with cholesterol. *J. Biol. Chem.* 1972;247(6):1918-1929.

48. Maxfield FR, Wüstner D. Analysis of cholesterol trafficking with fluorescent probes. *Methods Cell Biol.* 2012;108:367-393.

49. Svoboda MD, Christie JM, Eroglu Y, Freeman KA, Steiner RD. Treatment of Smith–Lemli–Opitz syndrome and other sterol disorders. *Am. J. Med. Genet. C Semin. Med. Genet.* 2012;160C(4):285-294.

50. Mukherjee S, Maxfield FR. Cholesterol: stuck in traffic. *Nat. Cell Biol.* 1999;1(2):E37-E38.

51. Mukherjee S, Maxfield FR. Lipid and cholesterol trafficking in NPC. *Biochim. Biophys. Acta* 2004;1685(1-3):28-37.

52. Wassif CA, Vied D, Tsokos M, Connor WE, Steiner RD, Porter FD. Cholesterol storage defect in RSH/Smith-Lemli-Opitz syndrome fibroblasts. *Mol. Genet. Metab.* 2002;75(4):325-334.

53. Funk RS, Krise JP. Cationic amphiphilic drugs cause a marked expansion of apparent lysosomal volume: Implications for an intracellular distribution-based drug interaction. *Mol. Pharm.* 2012;9(5):1384-1395.

54. Nezil FA, Bloom M. Combined influence of cholesterol and synthetic amphiphillic peptides upon bilayer thickness in model membranes. *Biophys. J.* 1992;61(5):1176-1183.

55. Bretscher MS, Munro S. Cholesterol and the golgi apparatus. *Science* 1993;261(5126):1280-1281.

56. Róg T, Vattulainen I, Jansen M, Ikonen E, Karttunen M. Comparison of cholesterol and its direct precursors along the biosynthetic pathway: effects of cholesterol, desmosterol and 7-dehydrocholesterol on saturated and unsaturated lipid bilayers. *J. Chem. Phys.* 2008;129(15):154508.

57. Ren G, Jacob RF, Kaulin Y, DiMuzio P, Xie Y, Mason RP, Tint GS, Steiner RD, Roullet J-B, Merkens L, Whitaker-Menezes D, Frank PG, Lisanti MP, Cox RH, Tulenko TN. Alterations in membrane caveolae and BK_{Ca} channel activity in skin fibroblasts in Smith–Lemli–Opitz syndrome. *Mol. Genet. Metab.* 2011;104(3):346-355.

58. Tulenko TN, Boeze-Battaglia K, Mason RP, Tint GS, Steiner RD, Connor WE, Labelle EF. A membrane defect in the pathogenesis of the Smith-Lemli-Opitz syndrome. *J. Lipid Res.* 2006;47(1):134-143.

59. Berring EE, Borrenpohl K, Fliesler SJ, Serfis AB. A comparison of the behavior of cholesterol and selected derivatives in mixed sterol–phospholipid Langmuir monolayers: a fluorescence microscopy study. *Chem. Phys. Lipids* 2005;136(1):1-12.

60. Shrivastava S, Paila YD, Dutta A, Chattopadhyay A. Differential effects of cholesterol and its immediate biosynthetic precursors on membrane organization. *Biochemistry* 2008;47(20):5668-5677.

61. Wolf C, Chachaty C. Compared effects of cholesterol and 7-dehydrocholesterol on sphingomyelin–glycerophospholipid bilayers studied by ESR. *Biophys. Chem.* 2000;84(3):269-279.

62. Staneva G, Chachaty C, Wolf C, Quinn PJ. Comparison of the liquid-ordered bilayer phases containing cholesterol or 7-dehydrocholesterol in modeling Smith-Lemli-Opitz syndrome. *J. Lipid Res.* 2010;51(7):1810-1822.

63. Haldar S, Kanaparthi RK, Samanta A, Chattopadhyay A. Differential effect of cholesterol and its biosynthetic precursors on membrane dipole potential. *Biophys. J.* 2012;102(7):1561-1569.

64. Singh P, Haldar S, Chattopadhyay A. Differential effect of sterols on dipole potential in hippocampal membranes: implications for receptor function. *Biochim. Biophys. Acta* 2013;1828(3):917-923.

65. Shrivastava S, Paila YD, Kombrabail M, Krishnamoorthy G, Chattopadhyay A. Role of cholesterol and its immediate biosynthetic precursors in membrane dynamics and heterogeneity: implications for health and disease. *J. Phys. Chem. B* 2020;124(29):6312-6320.

66. Mesmin B, Maxfield FR. Intracellular sterol dynamics. *Biochim. Biophys. Acta* 2009;1791(7):636-645.

67. Menon AK. Sterol gradients in cells. *Curr. Opin. Cell Biol.* 2018;53:37-43.

68. Sharpe HJ, Stevens TJ, Munro S. A comprehensive comparison of transmembrane domains reveals organelle-specific properties. *Cell* 2010;142(1):158-169.

69. Lebrand C, Corti M, Goodson H, Cosson P, Cavalli V, Mayran N, Fauré J, Gruenburg J. Late endosome motility depends on lipids via the small GTPase Rab7. *EMBO J.* 2002;21(6):1289-1300.

70. Sobo K, Le Blanc I, Luyet P-P, Fivaz M, Ferguson C, Parton RG, Gruenberg J, van der Goot FG. Late endosomal cholesterol accumulation leads to impaired intra-endosomal trafficking. *PLoS One* 2007;2(9)e851.

71. Pipalia NH, Hao M, Mukherjee S, Maxfield FR. Sterol, protein and lipid trafficking in Chinese hamster ovary cells with Niemann-Pick type C1 defect. *Traffic* 2007;8(2):130-141.

72. Choudhury A, Sharma DK, Marks DL, Pagano RE. Elevated endosomal cholesterol levels in Niemann-Pick cells inhibit rab4 and perturb membrane recycling. *Mol. Biol. Cell* 2004;15(10):4500-4511.

73. Bernier V, Lagacé M, Bichet DG, Bouvier M. Pharmacological chaperones: potential treatment for conformational diseases. *Trends Endocrinol. Metab.* 2004;15(5):222-228.

74. Dorsam RT, Gutkind JS. G-protein-coupled receptors and cancer. *Nat. Rev. Cancer* 2007;7(2):79-94.

75. Hollingsworth TJ, Gross AK. Defective trafficking of rhodopsin and its role in retinal degenerations. *Int. Rev. Cell Mol. Biol.* 2012;293:1-44.

76. Kumar GA, Chattopadhyay A. Statin-induced chronic cholesterol depletion switches GPCR endocytosis and trafficking: insights from the serotonin$_{1A}$ receptor. *ACS Chem. Neurosci.* 2020;11(3):453-465.

77. Roy S, Kumar GA, Jafurulla M, Mandal C, Chattopadhyay A. Integrity of the actin cytoskeleton of host macrophages is essential for *Leishmania donovani* infection. *Biochim. Biophys. Acta* 2014;1838(8):2011-2018.

78. Smith PK, Krohn RI, Hermanson GT, Mallia AK, Gartner FH, Provenzano MD, Fujimoto EK, Goeke NM, Olson BJ, Klenk DC. Measurement of protein using bicinchoninic acid. *Anal. Biochem.* 1985;150(1):76-85.

79. Bligh EG, Dyer WJ. A rapid method of total lipid extraction and purification. *Can. J. Biochem. Physiol.* 1959;37(8):911-917.

80. Aufenanger J, Pill J, Schmidt FH, Stegmeier K. The effects of BM 15.766, an inhibitor of 7-dehydrocholesterol Δ^7-reductase, on cholesterol biosynthesis in primary rat hepatocytes. *Biochem. Pharmacol*. 1986;35(6):911-916.

FIGURE LEGENDS

FIGURE 1 Generating a cellular model of Smith-Lemli-Opitz syndrome. (a) Two known pathways of cholesterol biosynthesis are the Kandutsch-Russell and the Bloch pathway. 7-DHC, the immediate biosynthetic precursor of cholesterol in the Kandutsch-Russell pathway, differs from cholesterol *merely* by the presence of an additional double bond (highlighted with a red circle). Mutation(s) in the enzyme (7-DHCR) catalyzing the conversion of 7-DHC to cholesterol leads to Smith-Lemli-Opitz syndrome, a metabolic disorder characterized by accumulation of 7-DHC and an altered cholesterol to total sterol ratio. We generated a cellular model of SLOS in HEK-5-HT_{1A}R cells (HEK-293 cells stably expressing N-terminal myc-tagged human serotonin$_{1A}$ receptors) using AY 9944, a metabolic inhibitor of 7-DHCR. (b) Viability of HEK-5-HT_{1A}R cells is not affected upon AY 9944 treatment. HEK-5-HT_{1A}R cells were treated with 2 and 4 μM AY 9944 for 66 h and cellular viability was measured using MTT assay. Values are expressed as percentage viability of cells treated with AY 9944 normalized to control (in the absence of AY 9944) cell. (c) Representative thin layer chromatogram showing lipids extracted from cell lysates prepared from HEK-5-HT_{1A}R control cells and treated with AY 9944. The chromatogram shows cholesterol and 7-DHC standards (lane 1), lipids extracted from cellular lysates under control (untreated, lane 2), and treated with 2 μM (lane 3) and 4 μM (lane 4) AY 9944. (d) Quantitation of the cholesterol/total sterol ratio (maroon, solid blue and solid green bars) and DHC/total sterol ratio (hatched blue and hatched green bars) was performed using densitometric analysis. Values are expressed as relative sterol content normalized to total sterol from corresponding samples in each case. Data represent means ± SEM from four independent experiments. See Materials and Methods for more details

FIGURE 2 Plasma membrane population of the serotonin$_{1A}$ receptor is reduced upon AY 9944 treatment without any change in its total cellular expression. (a) HEK-5-HT_{1A}R cells were treated with 2 and 4 μM AY 9944 for 66 h. Cells were subsequently fixed and labeled

with anti-myc antibody Alexa Fluor 488 conjugate. Overlays of representative flow cytometric histograms showing plasma membrane population of the serotonin$_{1A}$ receptor under control condition (maroon), and treated with 2 (blue) and 4 (green) μM AY 9944. The histogram corresponding to unstained cells (gray) is shown as reference. (b) Quantitative flow cytometric estimates of plasma membrane receptor population under these conditions. Values are normalized to mode count in control cells. Data represent means ± SEM from at least four independent experiments (*** represents a significant ($p < 0.001$) difference in mode count associated with AY 9944 treated cells relative to control cells). (c) Western blot showing total cellular expression of the serotonin$_{1A}$ receptor upon 2 and 4 μM AY 9944 treatment for 66 h. Corresponding β-tubulin expression levels are shown below as loading controls. (d) Total cellular expression of the serotonin$_{1A}$ receptor was analyzed using densitometric analysis and normalized to β-tubulin. Values are represented as percentage expression of the serotonin$_{1A}$ receptor normalized to control cells in each case. Data represent means ± SEM from four independent experiments. See Materials and Methods for more details

FIGURE 3 Increase in cellular LysoTracker positive compartments upon AY 9944 treatment. HEK-5-HT$_{1A}$R cells were treated with AY 9944 for 66 h and subsequently stained with 0.3 μM LysoTracker red at 37 °C for 30 min. (a) Representative confocal microscopic images of the mid-plane section showing LysoTracker red staining under control and 2 and 4 μM AY 9944 treatment conditions. (b) Overlays of representative flow cytometric histograms showing LysoTracker red stained population under control condition (maroon), and treated with 2 (blue) and 4 (green) μM AY 9944. The histogram corresponding to unstained cells (gray) is shown as a reference. (c) Total LysoTracker red positive population quantified using flow cytometry. Data represent mean fluorescence intensity in control, and 2 and 4 μM AY 9944 treatment conditions. Values are represented as percentages of mean fluorescence intensity normalized to control condition. Data represent means ± SEM from three independent experiments (*** represents a significant ($p < 0.001$) difference in percentage

mean fluorescence intensity associated with AY 9944 treated cells relative to control cells). The scale bars represent 10 μm. See Materials and Methods for more details

FIGURE 4 The serotonin$_{1A}$ receptor is trafficked to LysoTracker positive compartments upon AY 9944 treatment. HEK-5-HT$_{1A}$R cells were treated with AY 9944 for 66 h and subsequently stained with 0.3 μM LysoTracker red at 37 °C for 30 min. Cells were fixed, permeabilized and stained with anti-myc antibody Alexa Fluor 488 conjugate. (a) Representative confocal microscopic images of the mid-plane section showing colocalization between LysoTracker positive compartments (red) and serotonin$_{1A}$ receptors (green) under control, and 2 and 4 μM AY 9944 treatment conditions. The scale bars represent 10 μm. (b) Quantitative estimates of colocalization of the serotonin$_{1A}$ receptor with LysoTracker red, analyzed using Manders' colocalization coefficient (M). Data represent means ± SEM from 27 measurements from three independent experiments (*** represents a significant (p < 0.001) difference in Manders' colocalization coefficient associated with colocalization of the serotonin$_{1A}$ receptor with LysoTracker red upon AY 9944 treatment relative to control cells). See Materials and Methods for more details

FIGURE 5 LysoTracker positive compartments accumulated upon AY 9944 treatment are sterol-enriched. HEK-5-HT$_{1A}$R cells were treated with AY 9944 for 66 h and stained with 0.3 μM LysoTracker red at 37 °C for 30 min. Cells were subsequently fixed and stained with filipin. (a) Representative confocal microscopic images of the mid-plane section showing colocalization between LysoTracker positive compartments (red) and filipin (blue) under control, 2 and 4 μM AY 9944 treatment conditions. The scale bars represent 10 μm. (b) Quantitative estimates of colocalization of filipin with LysoTracker red, analyzed using Manders' colocalization coefficient. Data represent means ± SEM from 27 measurements from three independent experiments (*** represents a significant (p < 0.001) difference in Manders' colocalization coefficient associated with colocalization of filipin with LysoTracker

red upon AY 9944 treatment relative to control cells). See Materials and Methods for more details

FIGURE 6 SLOS-like conditions alter subcellular localization and trafficking of the serotonin$_{1A}$ receptor. A schematic representation showing localization of serotonin$_{1A}$ receptors under SLOS-mimicking conditions upon chronic treatment of cells stably expressing the receptors with AY 9944, a specific inhibitor of the enzyme 7-DHCR. A significant reduction in plasma membrane population of the serotonin$_{1A}$ receptors associated with enhanced colocalization with sterol-enriched LysoTracker positive compartments was observed under SLOS-mimicking conditions. Two putative mechanisms underlying the altered subcellular localization of the serotonin$_{1A}$ receptor in SLOS-like conditions are shown in a box on the far right: (i) receptors are targeted to these compartments during biosynthetic traffic (proposed pathway 1) instead of being sorted along the ER-Golgi-plasma membrane pathway, or (ii) serotonin$_{1A}$ receptors are routed toward LysoTracker positive compartments in the course of constitutive internalization and recycling to the plasma membrane (proposed pathway 2) (see text for other details)

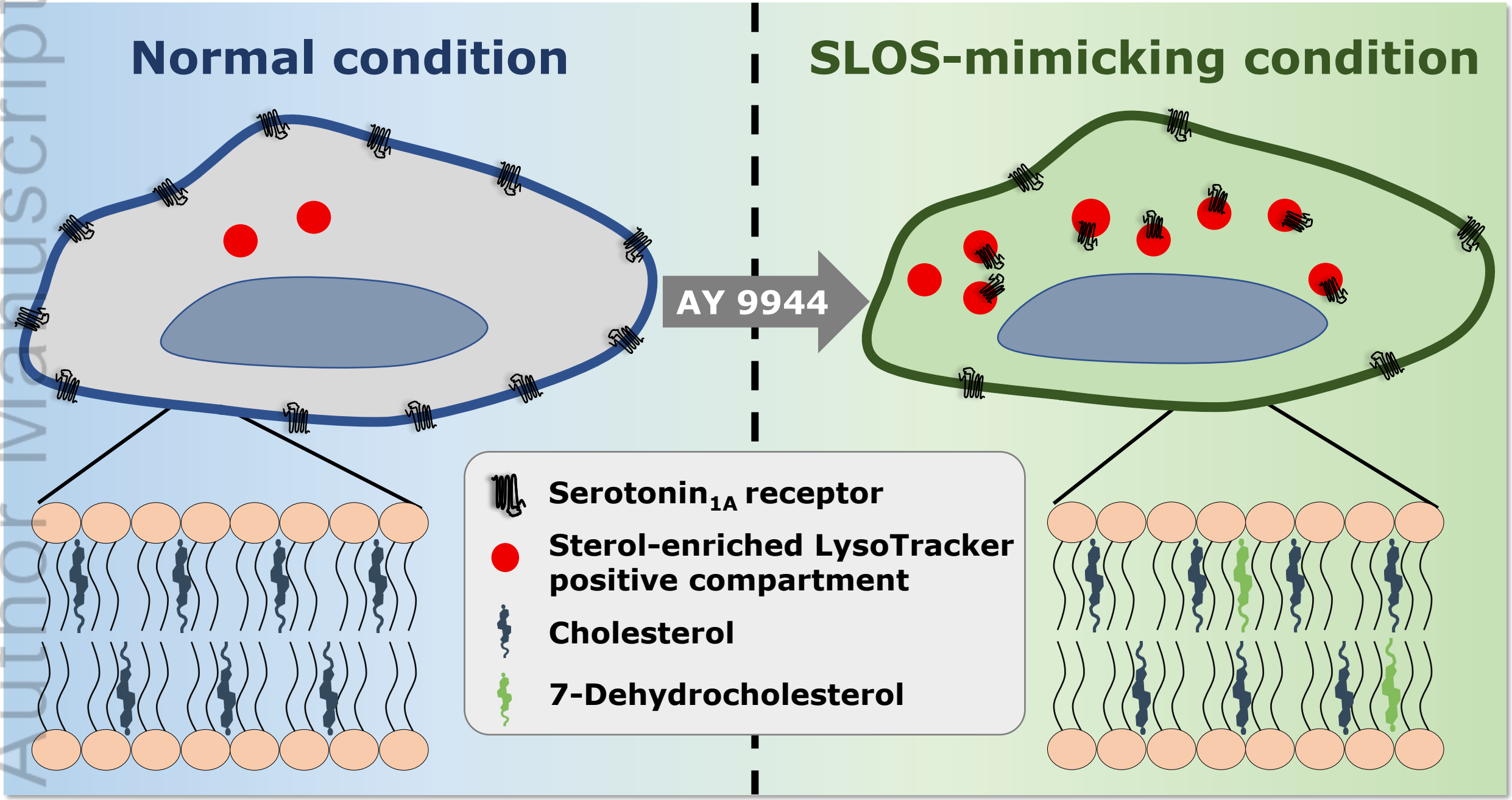

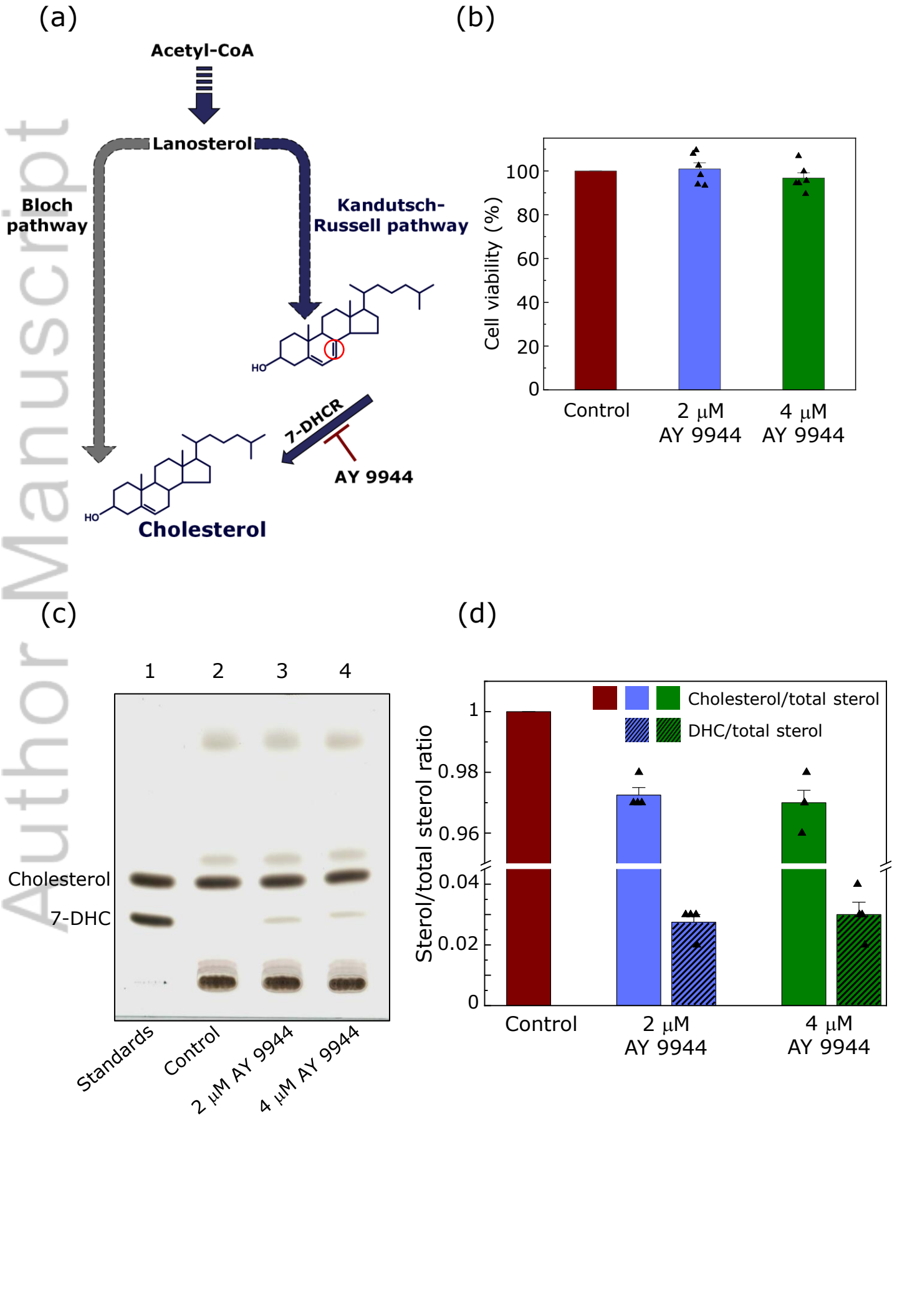

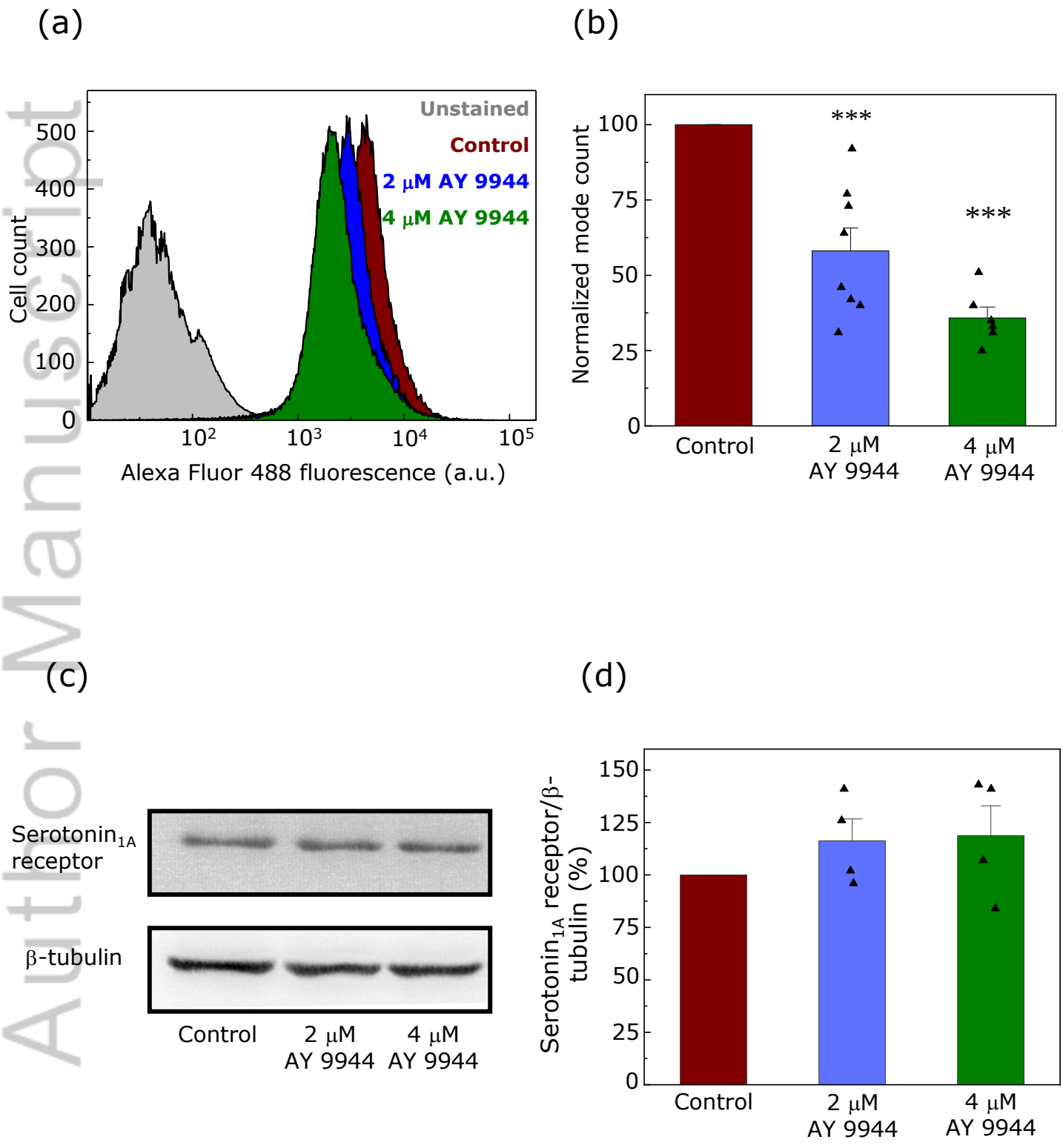

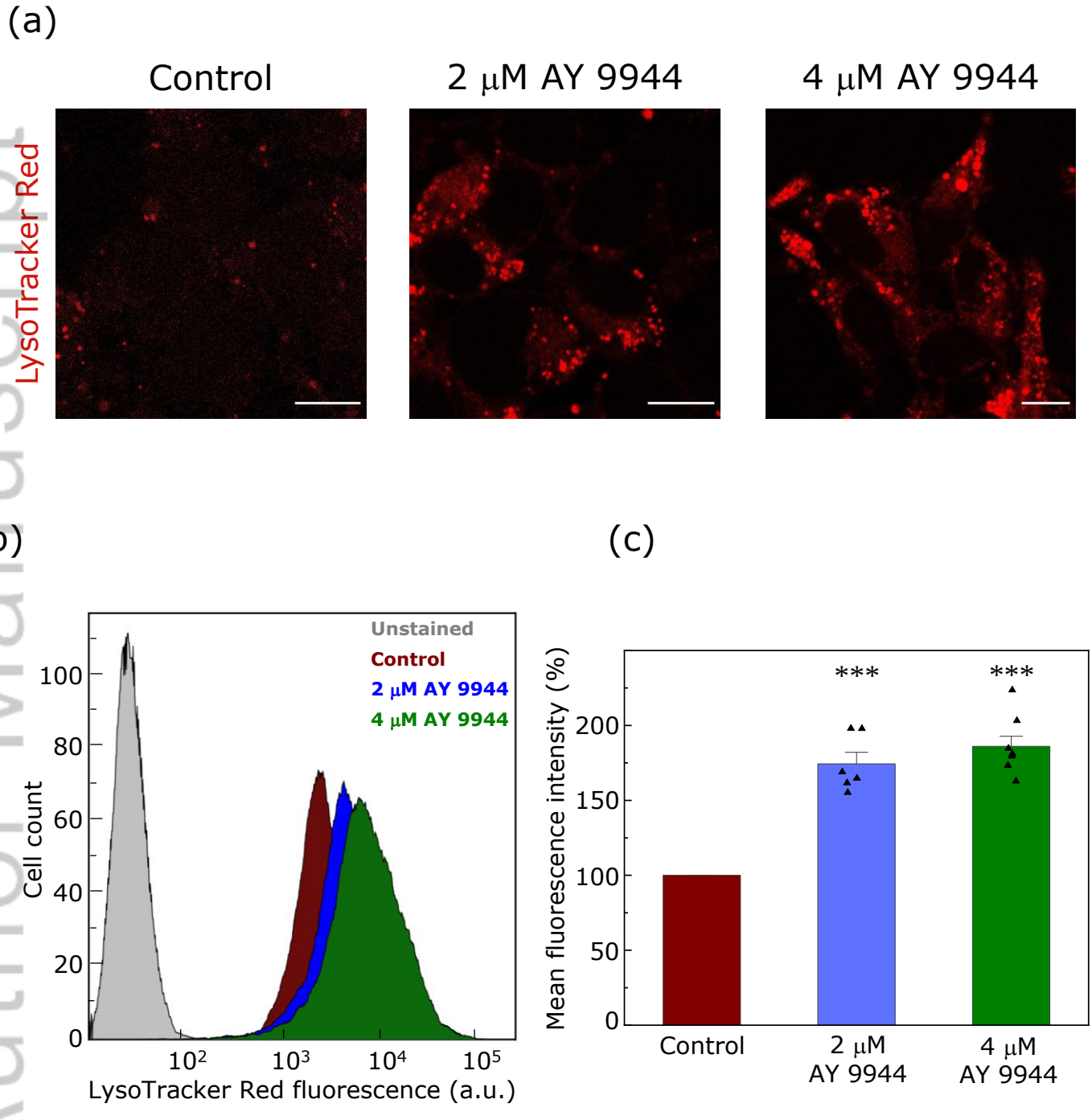

Figure 4
Sharma *et al.*

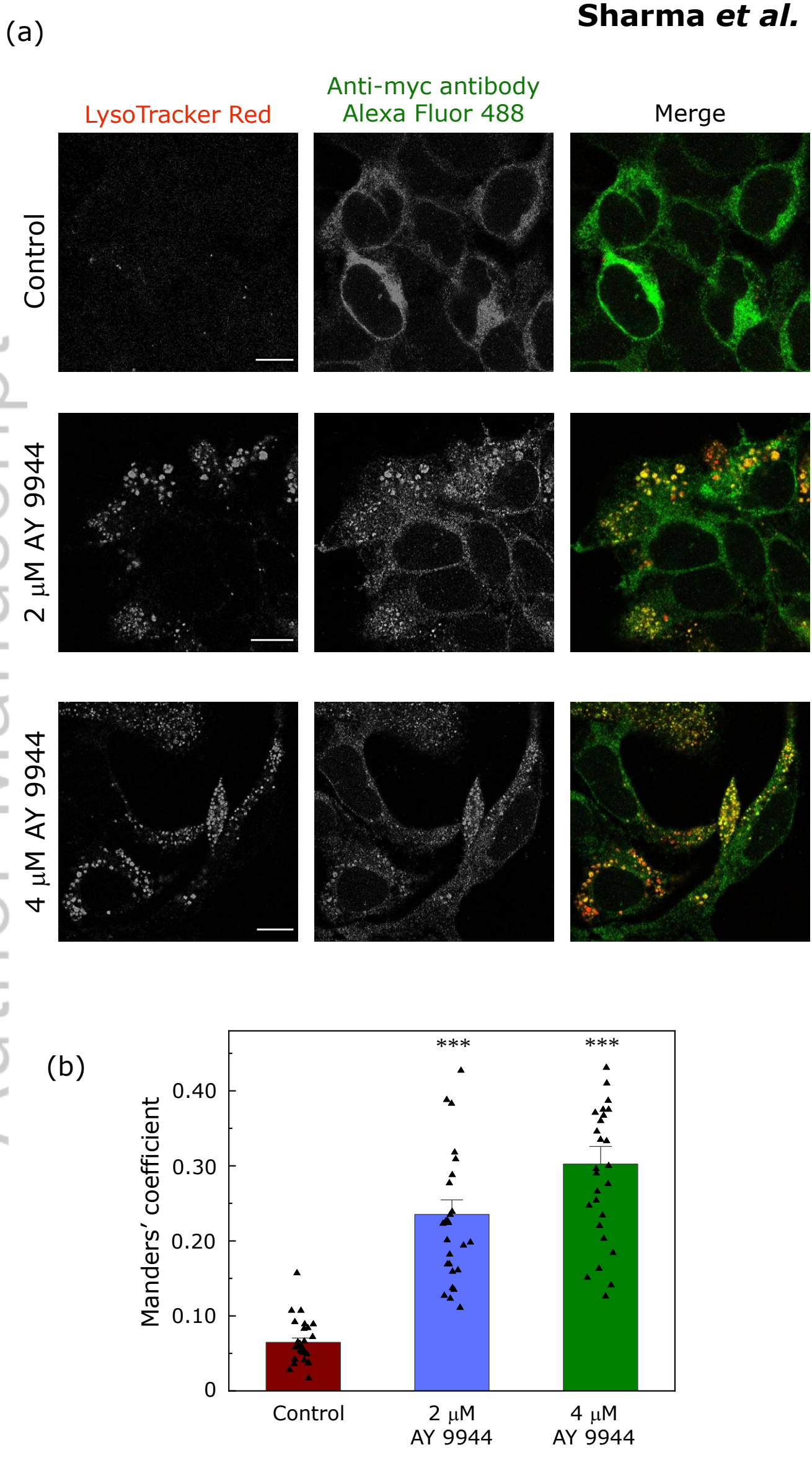

Figure 5
Sharma *et al.*

(a)

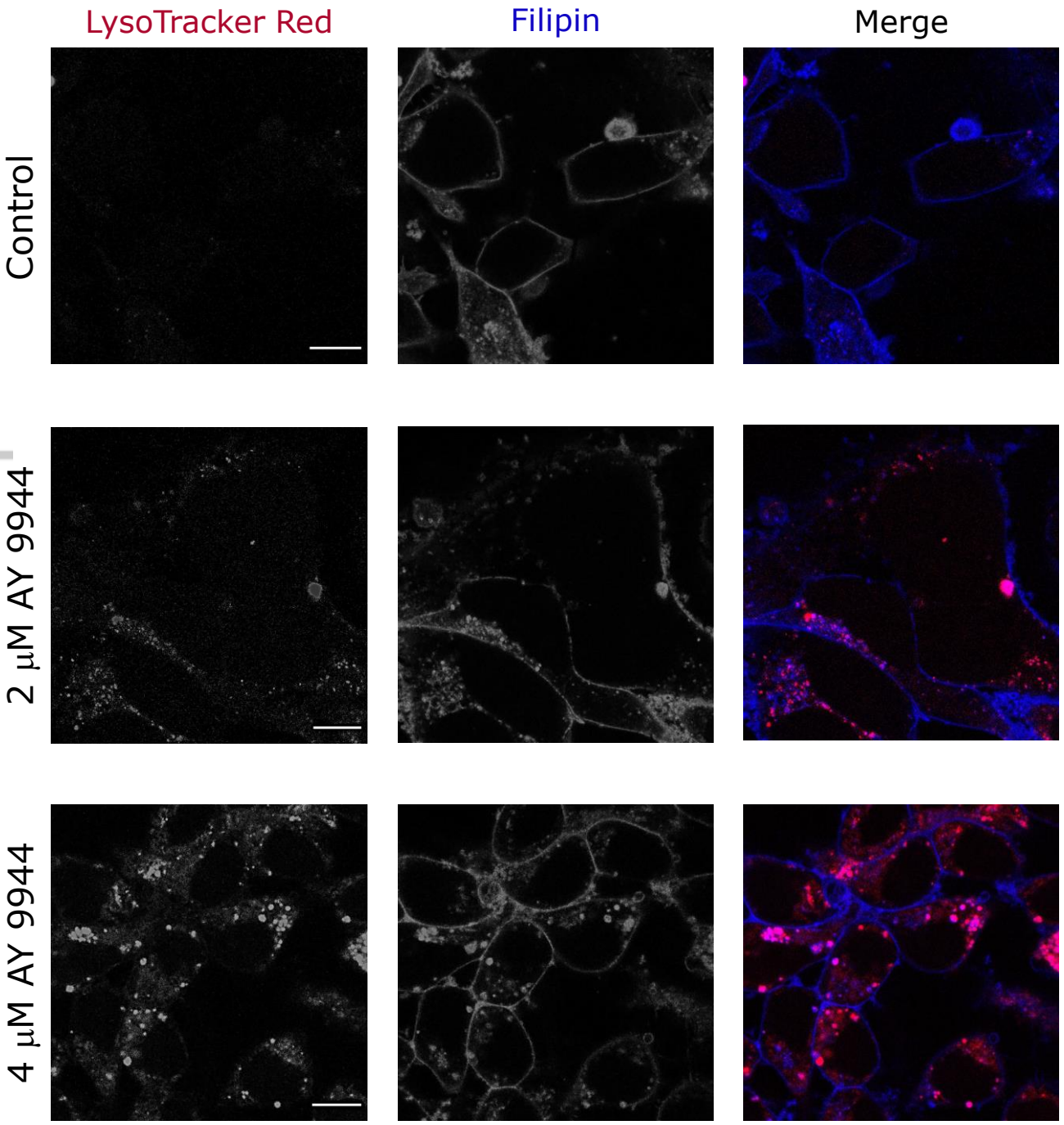

(b)

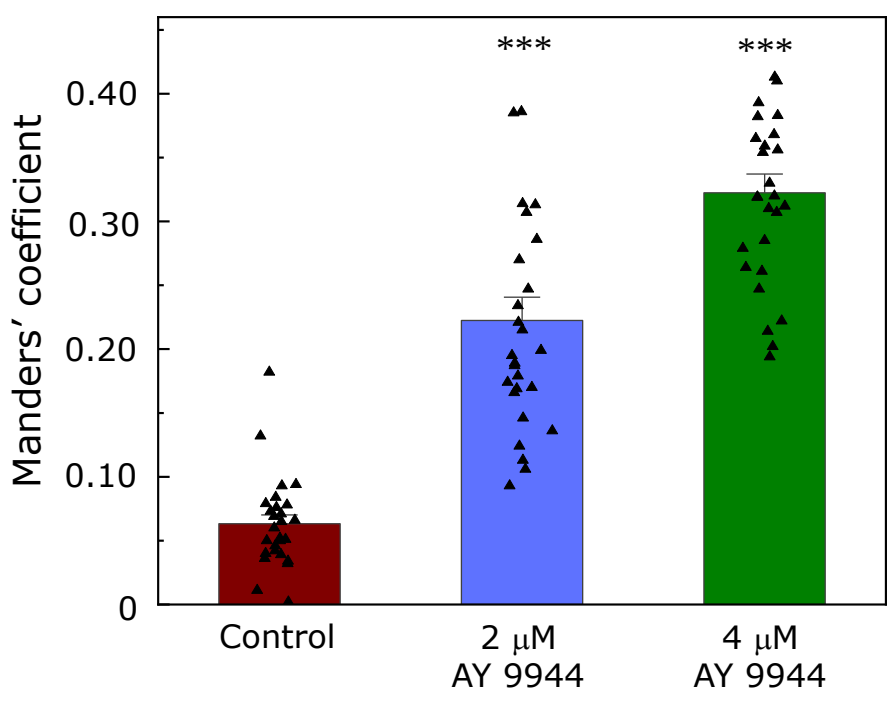

Figure 6
Sharma *et al.*